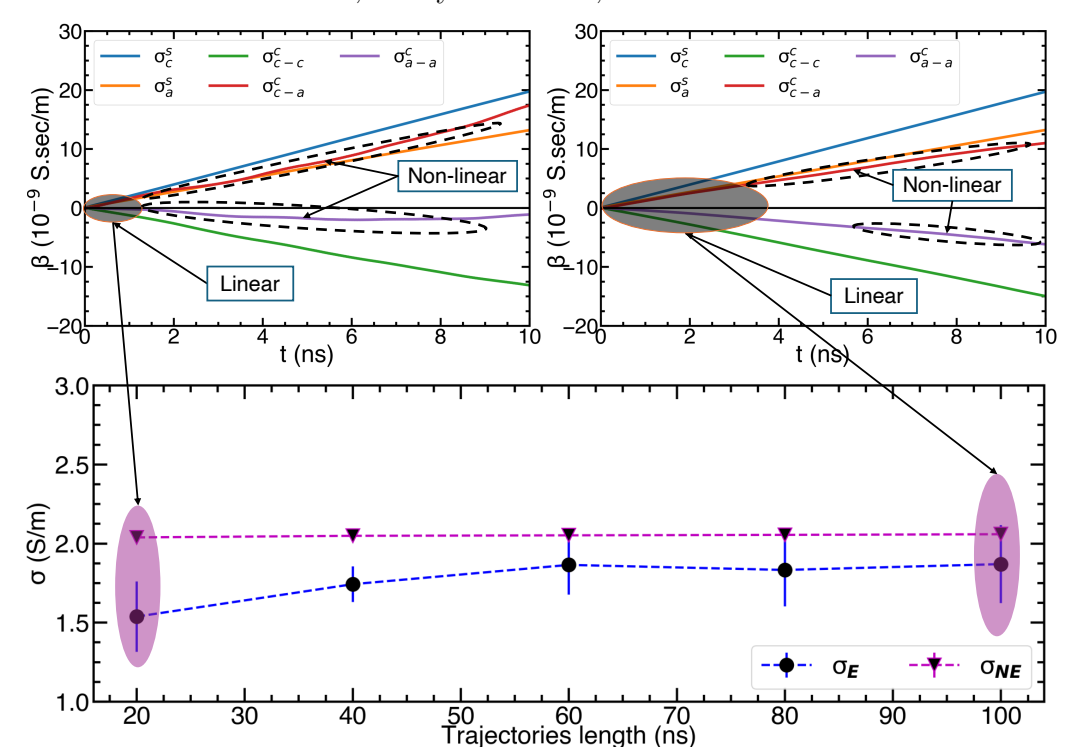
Graphical Abstract

Estimating Ionic Conductivity of Ionic Liquids: Nernst-Einstein and Einstein Formalisms

Ashutosh Kumar Verma, Amey S. Thorat, Jindal K. Shah



Highlights

Estimating Ionic Conductivity of Ionic Liquids: Nernst-Einstein and Einstein Formalisms

Ashutosh Kumar Verma, Amey S. Thorat, Jindal K. Shah

- Ionic conductivities in ionic liquids are calculated using Nernst-Einstein and Einstein formalisms.
- Challenges in estimating Einstein ionic conductivity using molecular simulations are identified.
- A workflow for calculating ionic conductivity using the Einstein formalism is developed.
- A simplified approach to reduce the computational cost of Einstein conductivity calculations is introduced.

Estimating Ionic Conductivity of Ionic Liquids: Nernst-Einstein and Einstein Formalisms

Ashutosh Kumar Verma^a, Amey S. Thorat^a, Jindal K. Shah^{a,*}

^aSchool of Chemical Engineering, Oklahoma State University, Stillwater, 70784, OK, United States

Abstract

Ionic conductivity plays an important role in the application of ionic liquids as electrolytes in next-generation batteries and electrochemical applications and is often estimated using the Nernst-Einstein formalism in molecular simulation-based studies. The Nernst-Einstein formalism is useful for dilute systems where ions do not interact with each other, restricting its applicability to infinitely diluted solutions. However, this approximation fails in concentrated solutions where ion interactions become significant, which is usually encountered for pure ionic liquids. These ion-ion correlations can dramatically affect ionic conductivity predictions in comparison to that computed under the Nernst-Einstein formalism. This study highlights the challenges associated with calculating ionic conductivity using Einstein formalism and subsequently provides a workflow for such calculations. It has been found that a minimum trajectory length of 60 ns is required to achieve converged results for Einstein ionic conductivity. Guidance is also given to reduce the computational resource requirements for Einstein conductivity determinations. This simplification will enable researchers to estimate Einstein conductivity in ionic liquids more efficiently.

Keywords: Einstein, Nernst-Einstein, Ionic liquids, Ionic conductivity, Ion correlations

Email address: jindal.shah@okstate.edu (Jindal K. Shah)

1. Introduction

Ionic liquids (ILs) are a promising solvent alternative to volatile organic solvents in the chemical and related industries [1, 2]. They offer numerous advantages, including low volatility [3], nonflammability, exceptional thermal and chemical stability [4], high solubility, significant ionic conductivity, and a wide electrochemical potential window. These unique properties make them ideal for various applications, such as electrolytic materials in electrochemical devices [5], solvents/adsorbents for capturing greenhouse gases like CO₂ [6, 7], and catalysts or synthesis solvents for metallic oxides [5, 8]. To explore the ILs application in electrochemical devices, it is crucial to have knowledge of the transport properties such as self-diffusion coefficient and ionic conductivity.

Since the beginning of the ionic liquid research, molecular simulationbased approaches have been applied for calculating various thermodynamic, transport, and structural properties. The popularity of this approach stems from the fact that potentially billions of ionic liquids are possible given the diversity of available cations, anions, and substituent groups to choose from. It would be nearly impossible to experimentally traverse such a vast chemical space to identify a candidate IL for a given application. Additionally, molecular simulation trajectories can be analyzed to offer molecular-level insight into various physical phenomena and even suggest new ionic liquids for synthesis and physical property characterization. A common method for calculating the transport coefficients, such as ionic conductivity, using molecular simulations, relies on the application of the Nernst-Einstein (NE) and Einstein formalism [9]. In the NE-based calculations, the movement of ions in the system is assumed to be uninfluenced by the presence of other ions. As this assumption does not take into account ion correlation, the ionic conductivity calculated with the NE equation leads to an upper bound for the ionic conductivity. It finds relevance in dilute solutions or systems where the approximation of ions moving independently of each other holds reasonably well [10]. On the other hand, the Einstein formalism is better suited for complex electrolyte systems or situations where ions interact strongly with each other or solvents. It takes into account the effects of ion-ion and ion-solvent interactions [11], which can significantly reduce the ionic conductivity [12] in comparison to that calculated using the NE approach.

Several studies have explored ionic conductivity using NE, which is straightforward to obtain when compared to estimating ionic conductivity using Einstein formalism as the NE conductivity can be calculated if self-diffusion coefficients of species are known. The ease of calculating the self-diffusion coefficient and NE conductivity lies in the nature of these properties and the underlying calculations involved. These properties are derived from the mean square displacement (MSD) of particles or ions in a system, which measures the average distance particles travel over a given time period. Analyzing the MSD, one can determine the diffusion coefficient and conductivity using relatively straightforward mathematical relations. These calculations are based on the assumption of a linear relationship between the MSD and time [13, 14].

The key step in calculating Einstein conductivity is evaluating the sum of dot products of positional vectors. This involves taking into account the relative positions and movements of the charged particles in the system. By considering these factors, one can determine the conductivity of the ILs. However, this process introduces additional complexity and computational challenges [15]. The computational cost increases significantly as the number of particles in the system is typically large, requiring efficient algorithms and computational resources. Moreover, accurately modeling the interactions between charged particles and incorporating the dynamics of the system can be challenging.

The recent work by France-Lanord and Grossman introduced a new approximation for ionic conductivity, specifically designed for dynamical atomicscale simulations and based on the NE equation. Their approach considers ionic aggregates as elementary charge carriers, treating them as noninteracting species. This strategy effectively accounts for the primary influence of ion-ion correlations on conductivity [9]. Additionally, the work by Kubisiak and Eilmes contributed to the understanding of ionic conductivity using Einstein formalism. Their findings suggest that approximately 40 independent MD simulations are necessary to effectively reduce errors in ionic conductivity [15]. Recently, Madrid and Delft group computed electrical conductivities under ambient conditions of aqueous NaCl and KCl solutions by using the Einstein-Helfand equation [16]. These approaches offer accurate estimates of ionic conductivity, but they come with certain limitations. The method by France-Lanord and Grossman requires knowledge of cluster information for ILs, which can be challenging to obtain. Meanwhile, the approach by Kubisiak and Eilmes demands a large number of simulation trajectories, leading to significant computational requirements. Thus, we need an alternative approach that requires less computational requirements and predicts more

reliable ionic conductivity using Einstein formalism.

Recently, Maginn et al. published "best practices" for computing selfdiffusion coefficients from equilibrium MD simulations [17]. Additionally, analysis tools like PyLAT have been developed for self-diffusivity and ionic conductivity [18]. However, despite the importance of the ionic conductivity of ionic liquids, a systematic pedagogical tool highlighting issues that may arise while calculating ionic conductivity and a protocol to efficiently compute ionic conductivity using the Einstein formalism is lacking. This article is an attempt to bridge this gap and is intended for those who are entering the field of molecular simulation of ionic liquids. The section "Theoretical Framework" provides a mathematical foundation for calculating ionic conductivity with the two approaches. Details of simulations are provided next, with an extensive discussion on the effect of the length of simulation and spacing of the simulation snapshots on the computed ionic conductivity. Based on these observations, a protocol for the calculation of ionic conductivity is recommended. The Conclusions section summarizes the work performed in this study and key observations.

2. Theoretical Framework

2.1. Nernst-Einstein Conductivity

The Nernst-Einstein ionic conductivity (σ), for a pure electrolyte, can be calculated from the knowledge of the self-diffusion coefficient of individual ions (Eq. 1)

$$\sigma_{\rm NE} = \frac{e^2}{V k_B T} (N_+ z_+^2 D_+ + N_- z_-^2 D_-)$$
 (1)

The above equation can be modified for mixtures as

$$\sigma_{\text{NE}} = \frac{e^2}{V k_B T} (N_1 z_1^2 D_1 + N_2 z_2^2 D_2 + \dots + N_n z_n^2 D_n) = \frac{e^2}{V k_B T} \sum_{i=1}^n N_i z_i^2 D_i$$
(2)

where e represents the elementary charge, V the volume of the system, k_B denotes the Boltzmann constant while T signifies the temperature of the system. The charges on the cation and anion are given by z_+ and z_- while the respective self-diffusion coefficients are labeled as D_+ and D_- ; N_+ and N_- indicate the number of cations and anions. N_i , z_i , and D_i are the number, charge, and self-diffusion coefficients of the i^{th} ion, respectively.

In an isotropic fluid, self-diffusion coefficient (D) for the ionic species of interest is obtained from the mean-squared displacement (MSD) over individual molecules (Eq. 3)

$$D_i = \frac{1}{6} \frac{d(MSD_i(t))}{dt} \tag{3}$$

The MSD, over a time interval t, is defined as

$$MSD_i(t) = \frac{1}{N_i} \left\langle \sum_{i=1}^{N_i} |r_i^{c}(t+t_0) - r_i^{c}(t)|^2 \right\rangle$$
 (4)

Here N_i denotes the number of ions, r_i^c is the location of the center of mass of the ions, and t_0 is the different time origins. The $\langle \ldots \rangle$ denotes that an ensemble average taken over these time origins. We suggest that the best practices article by Maginn et al. should be consulted for computing the diffusion coefficient using the MSD [17].

2.2. Einstein Conductivity

The NE equation is useful for dilute systems but is limited in accuracy due to its assumption of non-interacting ions, restricting its applicability to infinitely diluted solutions. However, this approximation fails in concentrated solutions where ion interactions become significant [19, 20, 21]. To obtain precise estimates of ionic conductivity in such systems, we must employ linear response theory [22] and derive an expression that accounts for ion correlations. The conductivity can be expressed using linear response theory and the Green-Kubo formalism [23]. According to this theory, it is represented as a time integral over the current-current auto-correlation function as:

$$\sigma = \frac{1}{3Vk_BT} \int_0^\infty dt \, \langle \vec{J}(t) \cdot \vec{J}(0) \rangle \tag{5}$$

where $\vec{J}(t)$ is the total current and given by

$$\vec{J}(t) = e \sum_{i=1}^{N} z_i(t) \vec{v}_i(t)$$
 (6)

where $\vec{v}_i(t)$ is the velocity of i^{th} ion and N is the total numbers of ions. Several challenges might be encountered when considering the long-time behavior of

the integral in the Green-Kubo formalism for conductivity. Molecular dynamics simulations are performed for a finite time, and the integral in the Green-Kubo formalism requires averaging over time-correlation functions until they have decayed significantly. Long-time correlations may require very long simulation times to capture accurately, which can be computationally expensive. The Green-Kubo formalism is derived under the assumption of the microcanonical ensemble. However, MD simulations often use other ensembles like the canonical or isothermal-isobaric ensemble. Thus, correctly accounting for ensemble effects is important for accurate results [24, 25]. Although not a significant challenge due to availability of abundant and relatively inexpensive storage, velocities are to be stored for computing conductivity using the Green-Kubo formalism. Using Einstein formalism, one can derive a precise expression for ionic conductivity that accounts for ion-ion correlations. Mathematically, Einstein conductivity is given by

$$\sigma = \lim_{t \to \infty} \frac{e^2}{6V t k_B T} \sum_{i,j} z_i z_j \langle [r_i^c(t+t_0) - r_i^c(t)] \cdot [r_j^c(t+t_0) - r_j^c(t)] \rangle$$
 (7)

Furthermore, the equation above can be separated into two components. The initial term can be expressed as a summation over individual MSD, resembling the Einstein equation for diffusion. The subsequent term represents the aggregate of cross terms, enabling the consideration of collective ion behavior within an electrolyte solution.

$$\sigma = \lim_{t \to \infty} \frac{e^2}{6Vtk_BT} \sum_{i} z_i^2 \langle [r_i^c(t+t_0) - r_i^c(t)]^2 \rangle + \lim_{t \to \infty} \frac{e^2}{3Vtk_BT} \sum_{i > i} z_i z_j \langle [r_i^c(t+t_0) - r_i^c(t)] \cdot [r_j^c(t+t_0) - r_j^c(t)] \rangle$$
(8)

Using the expression for self-diffusion coefficients (Eq. 3), the first term in the above equation can be recast in the form of self-diffusion coefficients of an ion of type k

$$\sigma = \frac{e^2}{Vk_B T} \sum_{k} N_k z_k^2 D_k + \lim_{t \to \infty} \frac{e^2}{3Vtk_B T} \sum_{i>j} z_i z_j \langle [r_i^c(t+t_0) - r_i^c(t)] \cdot [r_j^c(t+t_0) - r_j^c(t)] \rangle$$
(9)

The first term on the right-hand side of Eq. 9 contains only single-particle diffusion coefficients of species k. If the cross terms can be neglected, i.e., in very dilute solutions, the NE equation (Eq. 1) is recovered. The equation for computing self-diffusion coefficient (Eq. 4) and ionic conductivity (Eq. 7) requires the use of "unwrapped coordinates". That is, periodic boundary conditions should not be applied to the coordinates, the self-diffusivity and ionic conductivity will be underestimated. The below steps can be used to compute the ionic conductivity using Einstein formalism:

- 1. Obtain the center of mass data of ions or particles from simulations.
- 2. Apply time origin shifting and calculate the displacement of each ion by subtracting its current position $r_i^c(t+t_0)$ from positions $r_i^c(t)$.
- 3. Multiply the displacements with their corresponding charges.
- 4. Compute the dot product of the displacement vectors for ions i^{th} and j^{th} during the same time interval Δt .
- 5. Sum all the dot products and multiply the result by the factor $\frac{e^2}{6Vk_BT}$.
- 6. Plot the obtained values against t and determine the slope of the linear regions. The slope represents Einstein conductivity.

It is possible to further decompose Eq. 8 into contributions arising from different ion-ion correlations, i.e. for i = j and $i \neq j$. For example, in a pure IL, the number of the cations and anions are equal. Therefore, the total ionic conductivity of the IL can be written as

$$\sigma = \sigma_c^s + \sigma_a^s + \sigma_{c-c}^c + \sigma_{c-a}^c + \sigma_{a-a}^c \tag{10}$$

The self terms σ_c^s and σ_a^s arise from setting i=j and can be shown to lead to the Nernst-Einstein conductivity. On the other hand, three cross terms appears due to $i \neq j$: cation-cation (σ_{c-c}^c) , cation-anion (σ_{c-a}^c) , and anion-anion (σ_{a-a}^c) . We can calculate these components in a fashion analgous to that for overall ionic conductivity. We will show that a physically meaningful value of ionic conductivity depends on the behavior of the cross terms.

3. Computational Methods

3.1. Force Fields

We employed the virtual site OPLS force field, as proposed by Doherty et al. [26], to simulate imidazolium-based ILs. Nonbonded interactions

were modeled using the Lennard-Jones (LJ) 12-6 and electrostatic potential. Mathematically, the nonbonded potential can be expressed as follows:

$$U_{\text{nonbonded}} = \sum_{i=1}^{N_{\text{atoms}}} \sum_{j=1}^{i-1} \left[c \left(\frac{q_i q_j}{r_{ij}} \right) + 4\epsilon_{ij} \left(\left(\frac{\sigma_{ij}}{r_{ij}} \right)^{12} - \left(\frac{\sigma_{ij}}{r_{ij}} \right)^6 \right) \right]$$
(11)

where N_{atoms} denotes the number of atoms in the system, c is coulomb constant q_i and q_j are charges of i^{th} and j^{th} atoms, repsectively, σ_{ij} and ϵ_{ij} denote the LJ parameters for the cross interactions involving atoms i and j, and r_{ij} is the distance between these atoms. For unlike pair interactions, geometric combining rule was used for both the collision diameter and energy well depth, i.e., $\sigma_{ij} = (\sigma_{ii}\sigma_{jj})^{1/2}$ and $\epsilon_{ij} = (\epsilon_{ii}\epsilon_{jj})^{1/2}$. Nonbonded interactions were computed between molecules and intra-molecular atom pairs separated by three or more bonds while the 1-4 intramolecular nonbonded interactions were scaled by a factor of 0.5. For the calculation of the Lennard-Jone interactions, a cutoff of 13 Å was employed. Long-range corrections were applied to both energy and pressure. The electrostatic interactions were decomposed into short-range and long-range interactions, and a short-range electrostatics cutoff was set to 13 A. The short-range electrostatic interactions were computed by summing pair-wise interaction while Particle-Mesh Ewald summation was employed to account for long-range electrostatic interactions [27]. The equations of motion were integrated using the leap-frog algorithm with a time step of 1 fs. The LINCS algorithm was used to constrain the bonds involving hydrogen atoms [28].

3.2. Details of the MD Simulations Procedure

We considered widely used imidazolium-based ionic liquids: 1-ethyl-3-methylimidazolium tetrafluoroborate ($[C_2mim][BF_4]$), $[C_2mim]$ dicyanamide ($[C_2mim][DCA]$), $[C_2mim]$ bis(trifluoromethylsulfonyl)imide ($[C_2mim][NTF_2]$), and $[C_2mim]$ trifluoromethanesulfonate ($[C_2mim][TFO]$). MD simulations were conducted using GROMACS 4.5.5 software package [29]. Cubic boxes containing 500 ion pairs were generated using Packmol [30] with periodicity enforced along the three Cartesian axes. A simulation box of 500 ion pairs is shown in Figure 1(a). A series of steps was implemented to properly equilibrate each of the ionic liquid systems. First, we performed an energy minimization using the steepest descent algorithm for 5000 steps followed by a 1.5 ns annealing procedure. Starting at 0 K, the temperature was gradually raised to 313 K over 300 ps. It was then held at 313 K for 200 ps.

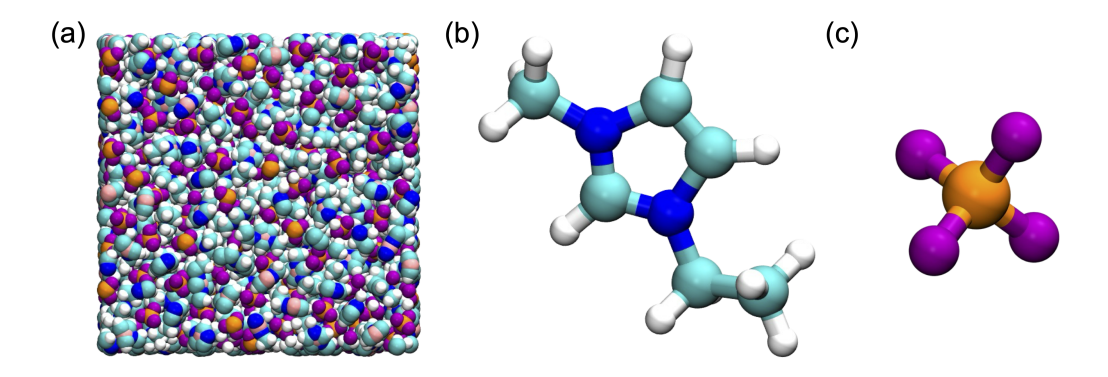


Figure 1: (a) A cubic simulation containing 500 ion pairs, (b) 1-ethyl-3-methylimidazolium $[C_2 \text{mim}]^+$ as the cation, and (c) $[BF_4]^-$ as an anion. The colors white, blue, cyan, orange, and violet represent hydrogen, nitrogen, carbon, boron, and fluorine atoms, respectively.

Subsequently, the temperature was further increased to 523 K over 200 ps and maintained at 523 K for 300 ps. Finally, it was lowered back to 313 K over 200 ps. Each system was then equilibrated in a canonical ensemble at 313 K for 5 ns. The temperature, in this phase, was controlled with a Berendsen thermostat with a time constant of 1 ps. [31] A 20 ns isothermalisobaric (NPT) simulation was then performed at 313 K and 1 bar. The temperature and pressure were maintained at the desired values using the v-scale thermostat [32] with a time constant of 1 ps and Berendsen barostat with a time constant of 1 ps. Subsequently, another 10 ns NPT equilibration run was performed using the Nosé-Hoover thermostat [33] (time constant of 2 ps) and Parrinello-Rahmanbarostat [34] (time constant of 10 ps). Finally, NPT production runs were carried out for 40 ns and 100 ns using the Nosé-Hoover thermostat (time constant of 2 ps) and Parrinello-Rahman barostat (time constant of 10 ps), and trajectory data were collected at every 1 ps and 5 ps for 40 ns and 100 ns, respectively. Three distinct initial configurations were generated using Packmol by varying the random seed. The reported averages and standard deviations of the simulated conductivity were calculated using these independent simulations. The entire simulation protocol is depicted in Figure 2.

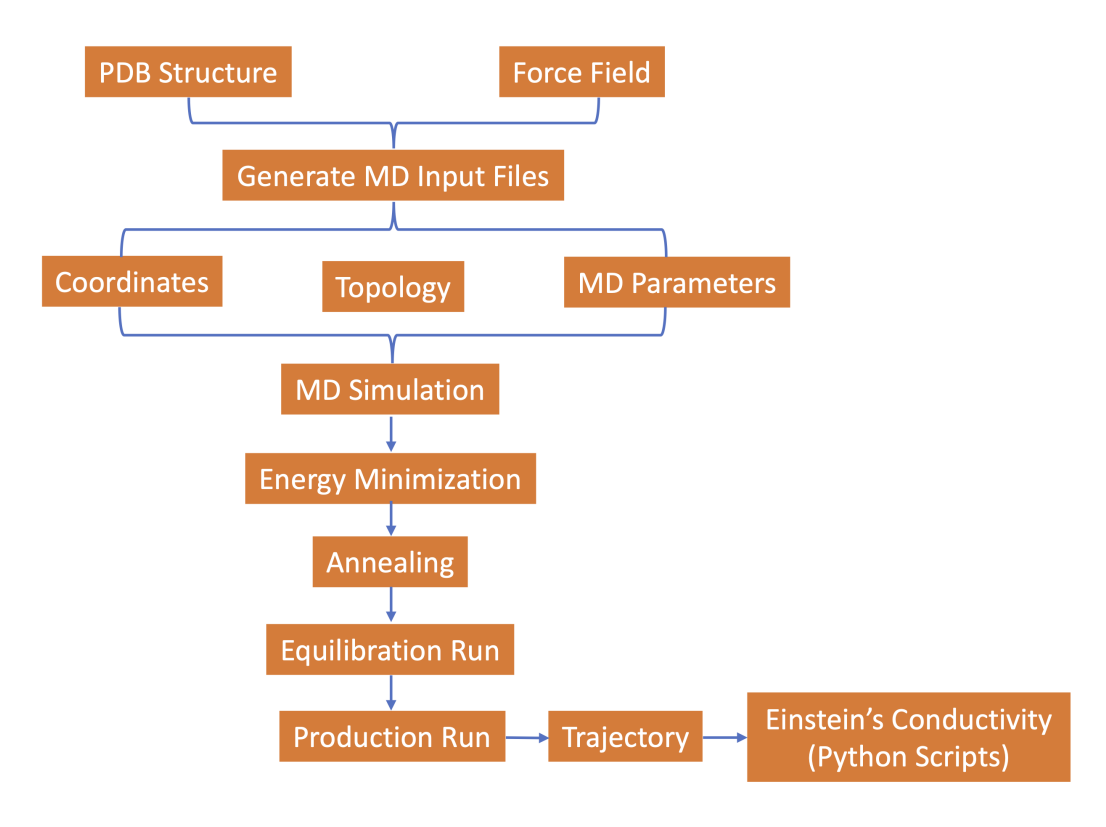


Figure 2: A simulation protocol showing key steps of Einstein conductivity using molecular simulation.

4. Results and Discussion

4.1. Nernst-Einstein and Einstein Conductivity

Figure 3 displays the NE and Einstein terms as a function of time for $[C_2 mim][BF_4]$ at 333 K for a time window up to 10 ns. Figure 3(a) was obtained by processing only the first 20 ns of the trajectory while the entire trajectory (100 ns) was used to calculate the NE and Einstein conductivity terms plotted in Figure 3(b). It can be clearly seen from both figures that the NE term remains linear over the entire 10 ns time window for both the trajectory lengths. On the other hand, considerable deviation from linearity is observed for the Einstein term. In fact, the linear behavior is maintained only over a short time window spanning 2 ns. It is this behavior that makes calculation of the ionic conductivity challenging requiring long simulation times for sluggish systems such as ionic liquids. The origin of the behavior stems from the number of samples available for averaging for the calculation

of NE and Einstein terms. For the former, as many samples as the number of ions in the system are available per snapshot while the collective nature of the Einstein term implies that only one sample can be obtained for averaging per simulation frame.

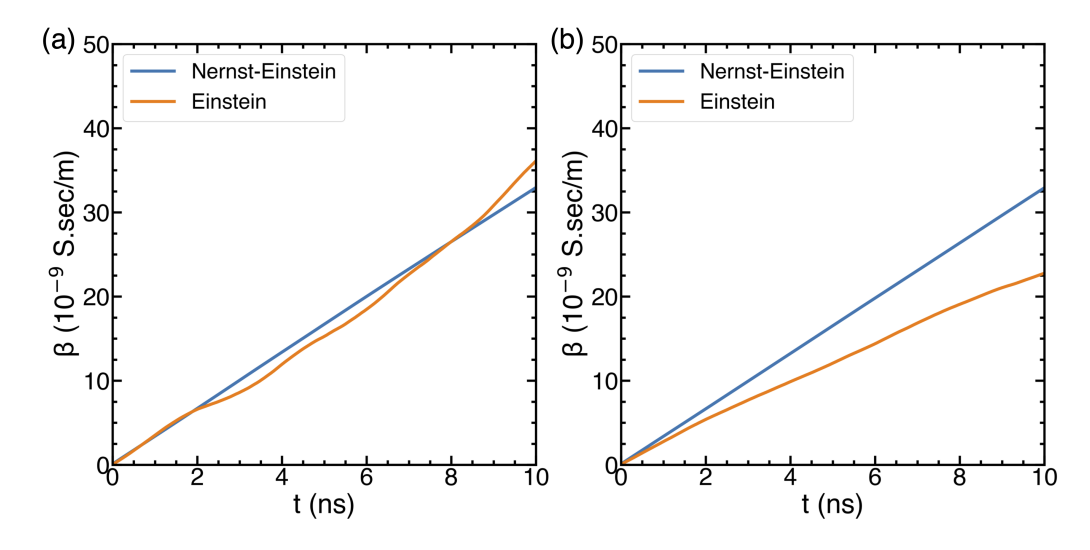


Figure 3: Nernst-Einstein and Einstein term for $[C_2mim][BF_4]$ at 333 K as a function of time. The length of the simulation trajectory is 20 ns (a) and 100 ns (b).

To glean additional insight into the behavior of the Einstein term over a short time window, we plotted both the NE and Einstein terms for time window up to 2 ns as shown in Figure 4, which demonstrates that the Einstein conductivity curve can exceed the NE conductivity curve for a shorter trajectory length. On the other hand, the Einstein conductivity curve remains below the NE conductivity curve for the entire 2 ns when a longer trajectory is employed as can be inferred from Figure 4(b). The effect of the contrasting behavior is reflected in the ionic conductivity calculated from the Einstein approach. For example, the ionic conductivity, based on the NE equation, yields a value of 3.24 S/m while an estimate of 3.47 S/m is obtained from the Einstein approach, which is unphysical. As the length of simulated trajectories is increased to 100 ns, the time window for computing Einstein conductivity also increases, resulting in a computed Einstein conductivity of 2.76 S/m, lower than the NE conductivity of 3.27 S/m. Our results indicate that it is important to calculate both the NE and the Einstein conductivity to ensure the physically expected behavior. In addition, it is imperative

to carry out long simulations of ionic liquids. In a later section, we revisit this issue and provide guidance on how long such simulations need to be to reliably compute the Einstein conductivity.

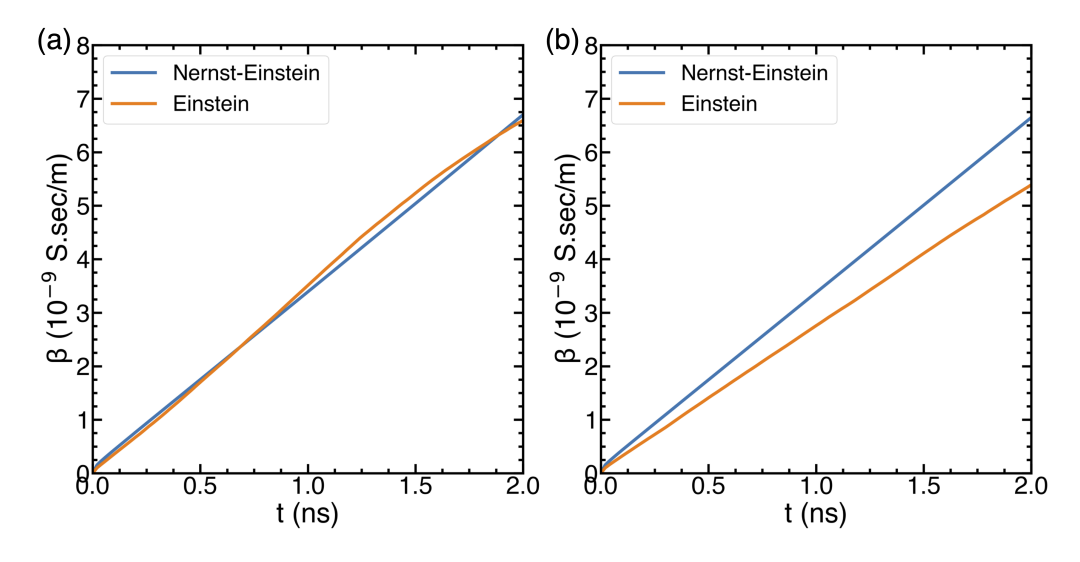


Figure 4: Nernst-Einstein and Einstein terms for $[C_2mim][BF_4]$ at 333 K as a function of time up to 2 ns time window. The length of the simulation trajectory is 20 ns (a) and 100 ns (b).

To trace the origin of the non-linear behavior of the Einstein term when a short simulation trajectory length is used, we decomposed the Einstein term into the self and cross terms (Eq. 9). We first analyzed the overall cross term comprising of the cation-cation, anion-anion, and cation-anion correlations. When plotted against the time for the first 10 ns as displayed in Figure 5, the self term that is related to the single particle diffusion shows a linear behavior as expected from Figures 5(a), irrespective of the length of the trajectory. In contrast, a highly non-linear, non-monotonic and oscillatory behavior with values taking both positive and negative values can be noted for the cross term for a trajectory length of 20 ns; extending the trajectory length to 100 ns results in a linear behavior up to 10 ns. Moreover, the crossterm was found to be a monotonically decreasing function with time, which is responsible for reducing the ionic conductivity from that computed using NE conductivity. The takeaway from this analysis is that it is necessary to examine the self and cross terms separately and ensure that both the terms are linearly correlated with time prior to computing the ionic conductivity

using the Einstein relation.

We also parsed the overall cross term into its individual components to

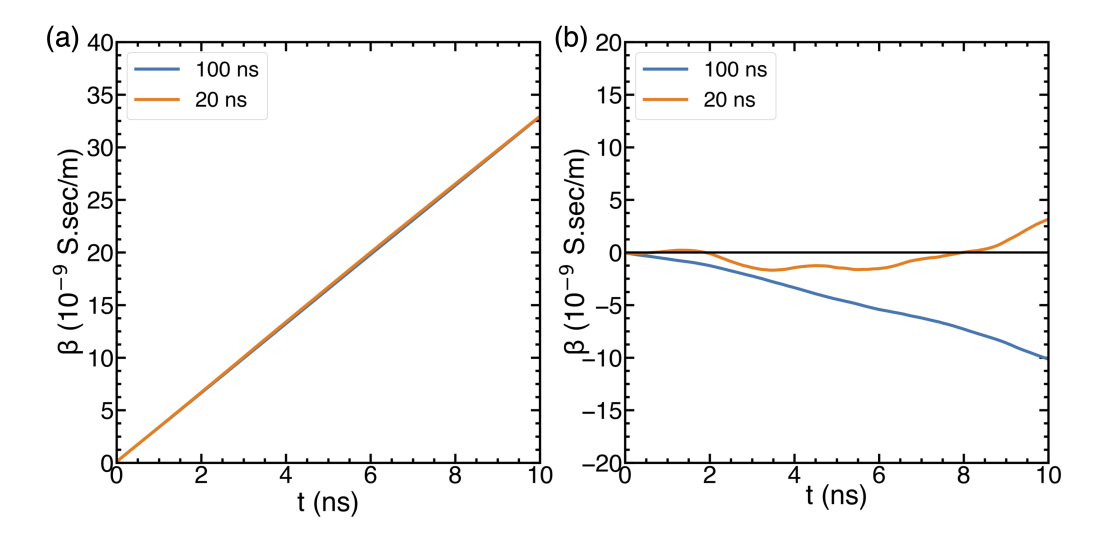


Figure 5: Conductivity terms obtained for a short (orange) and long (blue) trajectory for a time window of 10 ns, showing for (a) self terms and (b) cross terms.

determine correlation(s) responsible for the nonlinear behavior as depicted in Figure 6. An examination of the terms displayed in Figure 6(a), for a trajectory length of 20 ns, reveals that a pronounced curvature is present in the anion-anion correlation term, which contributes to the greatest extent in causing the non-linearity in the overall cross term, this is followed by the cation-anion correlation. The cation-cation correlation remains fairly linear over the first 10 ns time window. As opposed to these observations, all the components maintain linearity up to at least 10 ns for data extracted from a 100ns-long trajectory (Figure 6(b)).

4.2. Effect of Simulation Trajectory Length on the Ionic Conductivity

The above analysis suggests that the simulation should be conducted for greater than 20 ns and 100 ns long simulations appear to be adequate; however, it is not immediately apparent if any simulation less than 100 ns can be reliably employed for the ionic conductivity calculation. To answer this question, we examined Einstein conductivity of various systems ([C₂mim][BF₄], [C₂mim][DCA], [C₂mim][NTF₂], and [C₂mim][TFO]) at 313 K as shown in Figure 7. As we can see that the behavior of the Einstein curve varies among

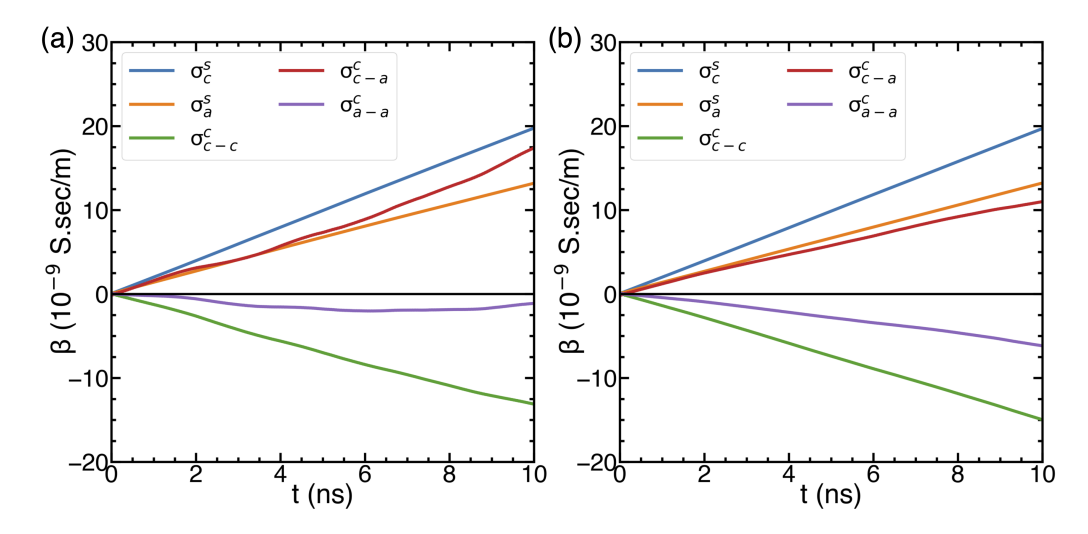


Figure 6: Self and cross correlation terms for the ionic liquid [C₂mim][BF₄] from a simulation conducted at 333 K. A trajectory length of 20 ns (a) and 100 ns (b) was used.

different systems and also changes with the trajectory's length. Initially, these curves for different trajectory lengths showed linear trends, but they started to diverge as time progressed, with noticeable differences after 5 ns. As expected, the longer the simulation trajectory, the longer the time window over which the linearity persists. Thus, the conductivity curve exhibits the most linearity trends within the first 1-2 ns, as seen in Figure 7. Therefore, a time window of at least 1-2 ns is recommended for Einstein conductivity calculations. Figure 8 depicts the ionic conductivity of $[C_2 mim][BF_4]$, [C₂mim][DCA], [C₂mim][NTF₂], and [C₂mim][TFO] at 313 K with varying trajectory lengths. For the ionic liquids [C₂mim][BF₄] and [C₂mim][DCA] (Figures 8(a) and 8(b)), with an increase in the length of trajectories, the Einstein conductivity begins to rise, and it converges for [C₂mim][BF₄] at trajectory lengths of 60 ns or more and for [C₂mim][DCA] at 80 ns or more. For the ionic liquid $[C_2mim][NTF_2]$ (Figure 8(c)), the Einstein conductivity appears to remain constant except for a slight drop at 40 ns. Finally, the Einstein ionic conductivity decreases with an increase in the length of the trajectory before leveling off for trajectories that are 60 ns and longer ([C₂mim][TFO], Figure 8(d)). These findings emphasize the variability in behavior and dynamics, highlighting the need for longer simulation trajectories to ensure accurate conductivity predictions. Therefore, it is essential to consider extended simulation trajectories (60 ns or more) when studying ionic

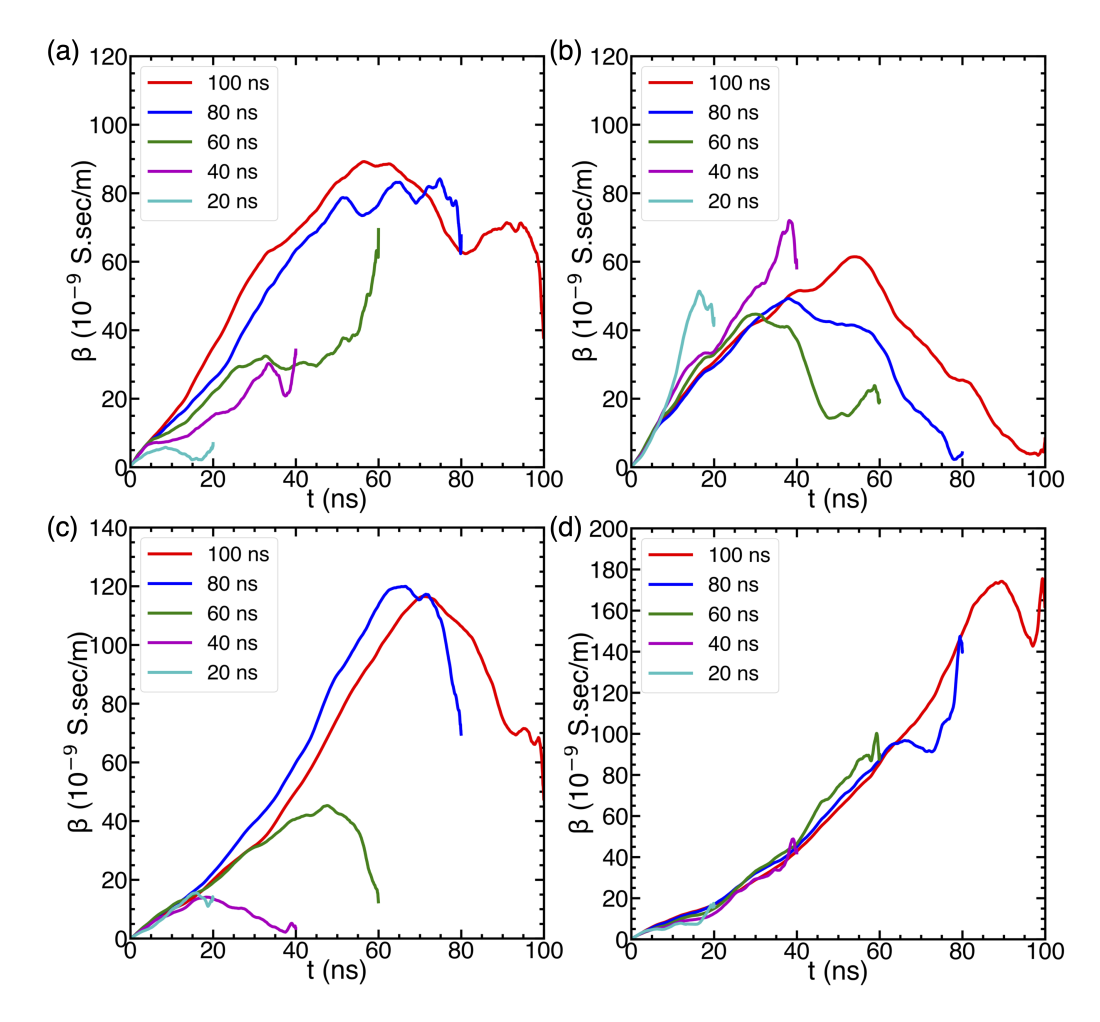


Figure 7: Showing Einstein terms obtained at 313 K with different trajectory lengths (a) [C₂mim][BF₄], (b) [C₂mim][DCA], (c) [C₂mim][NTF₂] and (d) [C₂mim][TFO].

liquid conductivity using the Einstein formalism. Figures 8 compare the calculated ionic conductivity from our simulations with experimental data from the literature [35, 36, 37, 38, 39, 40]. However, due to the inherent sensitivity of molecular simulations to force field parameters, absolute values of ionic conductivity may not perfectly match experimental results. Consequently, evaluating the accuracy of our methodology should not solely rely on this comparison.

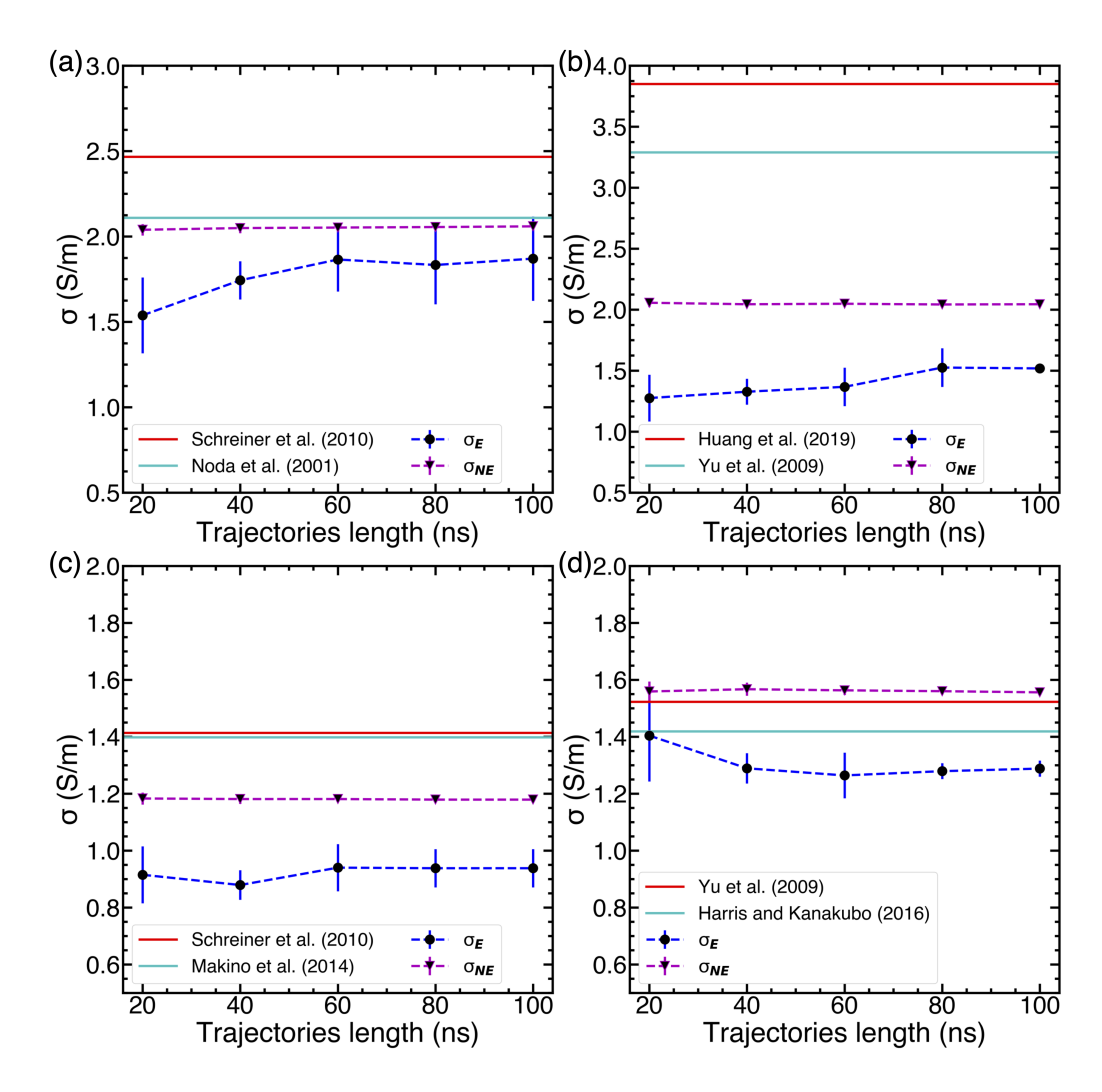


Figure 8: Ionic conductivity values for various trajectory lengths computed for a time windows of 1 ns at 313 K (a) $[C_2 mim][BF_4]$, (b) $[C_2 mim][DCA]$, (c) $[C_2 mim][NTF_2]$, and (d) $[C_2 mim][TFO]$. Dashed lines only act as visual guides.

4.3. Computational Resources Requirement

Calculating ionic conductivity using Einstein formalism can be challenging and computationally intensive, particularly when incorporating time origin shifting [18]. The process involves monitoring ion positions and their displacements in MD simulations. To increase the number of data points that can be used for averaging, time-origin shifting is recommended. However, im-

plementing time origin shifting requires multiple displacement calculations with different starting points, increasing computational resource demands. In this section, we explore an approach to reduce computational resource requirements by analyzing how frequently trajectories are to be stored without losing accuracy in calculating ionic conductivity.

Figure 9(a) depicts the ionic conductivity of $[C_2mim][BF_4]$ for a 40 ns

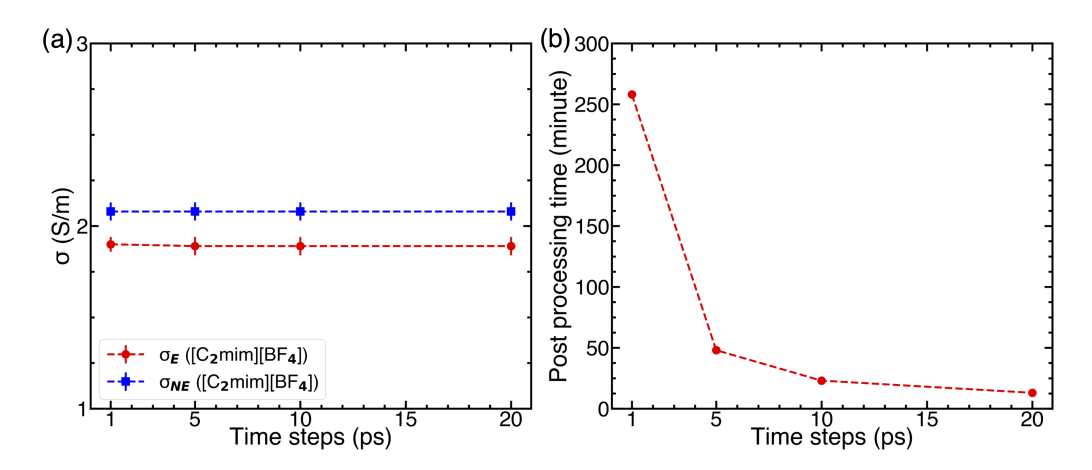


Figure 9: Showing (a) Conductivity values computed for a time windows of 1 ns and (b) post-processing time for a simulation trajectory printed at various time steps. A trajectory length of 40 ns was used. The dashed lines are only to act as a visual guide.

long simulation trajectory stored at an interval of 1 ps, 5 ps, 10 ps, and 20 ps. It can be readily observed that the value of ionic conductivity remains unaffected by the frequency at which snapshots are stored. This observation suggested that the storage requirements can be significantly reduced. Although the cost of storage has dramatically reduced over the years, it is still a consideration if a high-throughput screening of ionic liquids is to be carried out. Furthermore, reducing the number of time origin leads to proportionate reduction in the computational requirements as demonstrated in Figure 9(b).

5. Conclusions

The article focused on issues that emerge while calculating the ionic conductivity for ionic liquids using the Einstein formalism and presented several recommendations that can be followed to ensure reliable results from molecular simulations. Specifically, we demonstrated that a shorter simulation time

can lead to the Einstein conductivity greater than that predicted by the Nernst-Einstein formalism, which is physically unrealistic given that the ionion correlations in ionic liquids contribute rather significantly. To understand the origin of this behavior, an analysis of the terms that correspond to the ion diffusion and ion correlation was carried out which indicated that short simulations (20 ns in length) result in nonlinearities in the ion-ion correlation terms. Extending the simulation length to 100 ns resulted in correlation terms maintaining a linear behavior up to 10 ns. Therefore, we recommend that the averaging be carried out over the first 2 ns. While the evolution of these inter-ionic terms differs for every system, it is recommended that trajectories spanning 60-100 ns or longer be used to obtain a sufficiently long window over which the correlation term can be considered linear. Estimating Einstein conductivity using long trajectories can pose computational challenges pertaining to memory and storage. This issue can be resolved by recording the trajectory less frequently, such as every 20 ps. We also recommend to use the form of Einstein conductivity based on the overall dipole of the system to further increase computational efficiency. Avenues for future work include investigating the spatial decomposition of ion-ion correlations in ionic liquids that could help researcher to understand the effect of the neighboring and distant ions on correlations. Such insight could assist in the design of high conductivity ionic liquids where either there is a cancellation in the correlated motion or correlations are small. The approach outlined here should also provide a framework to ensure converged ionic conductivity in ionic liquid-salt mixtures where salt concentrations are low. In such cases, it would be important to ensure that cross-correlation terms involving dilute species (salts) are linear.

Conflicts of interest

Authors declare no conflict of interest.

Acknowledgement

The work performed for this publication was partially funded by the National Science Foundation grant OIA-1929163. The computing for this project was performed at the High Performance Computing Center at Oklahoma State University supported in part through the National Science Foundation grant OAC-1531128.

Data availability

All data used to support the findings of the study are included in the article.

Appendix A. Appendix

Here we show how to recast the original Einstein conductivity relationship so that the Eq. 7 in terms of time correlations of the simulation dipole. Starting with the expression of the ionic conductivity (Eq. 7)

$$\sigma = \lim_{t \to \infty} \frac{e^2}{6Vtk_BT} \sum_{i,j} z_i z_j \langle [r_i^c(t) - r_i^c(0)] \cdot [r_j^c(t) - r_j^c(0)] \rangle$$

Let's focus on the dot product inside the summation

$$\sum_{i,j} z_i z_j \langle [r_i^c(t) - r_i^c(0)] \cdot [r_j^c(t) - r_j^c(0)] \rangle$$

$$= \sum_{i,j} \langle [z_i r_i^c(t) - z_i r_i^c(0)] \cdot [z_j r_j^c(t) - z_j r_j^c(0)] \rangle$$
(A.1)

Defining $X_i^c = z_i r_i^c(t) - z_i r_i^c(0)$, and $X_j^c = z_j r_j^c(t) - z_j r_j^c(0)$, Eq. A.1 can be written as

$$\sum_{i,j} \langle [z_i r_i^c(t) - z_i r_i^c(0)] \cdot [z_j r_j^c(t) - z_j r_j^c(0)] \rangle = \sum_{i,j} \langle [X_i^c] \cdot [X_j^c] \rangle$$
 (A.2)

Expansion of the above equation leads to

To simplify the above expression, we consider a system consisting of only two ions,

$$\sum_{i,j} \langle [X_i^c] \cdot [X_j^c] \rangle = X_1^c \cdot X_1^c + X_1^c \cdot X_2^c + X_2^c \cdot X_1^c + X_2^c \cdot X_2^c$$
 (A.3)

The right hand side of the above equation can be simplified to a dot product of sum of X_1^c and X_2^c

$$X_1^c \cdot X_1^c + X_1^c \cdot X_2^c + X_2^c \cdot X_1^c + X_2^c \cdot X_2^c = (X_1^c + X_2^c) * (X_1^c + X_2^c)$$
 (A.4)

$$X_1^c + X_2^c = (z_1 r_1^c(t) - z_1 r_1^c(0)) + (z_2 r_2^c(t) - z_2 r_2^c(0))$$
(A.5)

Collecting terms with time t and 0,

$$X_1^c + X_2^c = (z_1 r_1^c(t) + z_2 r_2^c(t)) - (z_1 r_1^c(0) + z_2 r_2^c(0))$$
(A.6)

Therefore,

$$X_1^c + X_2^c = \sum_{i} z_i r_i^c(t) - \sum_{i} z_i r_i^c(0)$$
 (A.7)

In an analogous fashion, it can be shown that Eq. A.2 can be written

$$\sum_{i,j} \langle [z_i r_i^c(t) - z_i r_i^c(0)] \cdot [z_j r_j^c(t) - z_j r_j^c(0)] \rangle
= \left[\sum_i z_i r_i^c(t) - \sum_i z_i r_i^c(0) \right] \cdot \left[\sum_i z_i r_i^c(t) - \sum_i z_i r_i^c(0) \right]$$
(A.8)

Note that $\sum_{i} z_i r_i^c$ is the dipole moment of the simulation box. Therefore, the Einstein ionic conductivity expression, in terms of the dipole moment of the box, is

$$\sigma = \lim_{t \to \infty} \frac{e^2}{6Vtk_BT} \left\langle \left[\sum_i z_i r_i^c(t) - \sum_i z_i r_i^c(0) \right] \cdot \left[\sum_i z_i r_i^c(t) - \sum_i z_i r_i^c(0) \right] \right\rangle$$
(A.9)

References

- [1] E. Rezabal, T. Schäfer, Ionic liquids as solvents of polar and non-polar solutes: affinity and coordination, Physical Chemistry Chemical Physics 17 (22) (2015) 14588–14597.
- [2] M. J. Earle, K. R. Seddon, Ionic liquids. green solvents for the future, Pure and applied chemistry 72 (7) (2000) 1391–1398.

- [3] M. J. Earle, J. M. Esperança, M. A. Gilea, J. N. Canongia Lopes, L. P. Rebelo, J. W. Magee, K. R. Seddon, J. A. Widegren, The distillation and volatility of ionic liquids, Nature 439 (7078) (2006) 831–834.
- [4] J. S. Wilkes, M. J. Zaworotko, Air and water stable 1-ethyl-3-methylimidazolium based ionic liquids, Journal of the Chemical Society, Chemical Communications (13) (1992) 965–967.
- [5] M. Ue, M. Takeda, Application of ionic liquids based on 1-ethyl-3-methylimidazolium cation and fluoroanions to double-layer capacitors, J. Korean Electrochem. Soc 5 (2002) 192–196.
- [6] M. C. Corvo, J. Sardinha, T. Casimiro, G. Marin, M. Seferin, S. Einloft, S. C. Menezes, J. Dupont, E. J. Cabrita, A rational approach to co₂ capture by imidazolium ionic liquids: Tuning co₂ solubility by cation alkyl branching, ChemSusChem 8 (11) (2015) 1935–1946.
- [7] X. Zhang, X. Zhang, H. Dong, Z. Zhao, S. Zhang, Y. Huang, Carbon capture with ionic liquids: overview and progress, Energy & Environmental Science 5 (5) (2012) 6668–6681.
- [8] D. R. MacFarlane, N. Tachikawa, M. Forsyth, J. M. Pringle, P. C. Howlett, G. D. Elliott, J. H. Davis, M. Watanabe, P. Simon, C. A. Angell, Energy applications of ionic liquids, Energy & Environmental Science 7 (1) (2014) 232–250.
- [9] A. France-Lanord, J. C. Grossman, Correlations from ion pairing and the nernst-einstein equation, Physical review letters 122 (13) (2019) 136001.
- [10] L. Garrido, I. Aranaz, A. Gallardo, C. García, N. García, E. Benito, J. Guzmán, Ionic conductivity, diffusion coefficients, and degree of dissociation in lithium electrolytes, ionic liquids, and hydrogel polyelectrolytes, The Journal of Physical Chemistry B 122 (34) (2018) 8301– 8308.
- [11] J. O. Bockris, A. K. Reddy, J. O. Bockris, A. K. Reddy, Ion—ion interactions, Modern Electrochemistry: An Introduction to an Interdisciplinary Area Volume 1 (1970) 225–359.
- [12] Y. Marcus, G. Hefter, Ion pairing, Chemical reviews 106 (11) (2006) 4585–4621.

- [13] M. Kowsari, S. Alavi, M. Ashrafizaadeh, B. Najafi, Molecular dynamics simulation of imidazolium-based ionic liquids. i. dynamics and diffusion coefficient, The Journal of chemical physics 129 (22) (2008).
- [14] M. Kowsari, S. Alavi, M. Ashrafizaadeh, B. Najafi, Molecular dynamics simulation of imidazolium-based ionic liquids. ii. transport coefficients, The Journal of Chemical Physics 130 (1) (2009).
- [15] P. Kubisiak, A. Eilmes, Estimates of electrical conductivity from molecular dynamics simulations: How to invest the computational effort, The Journal of Physical Chemistry B 124 (43) (2020) 9680–9689.
- [16] S. Blazquez, J. L. Abascal, J. Lagerweij, P. Habibi, P. Dey, T. J. Vlugt, O. A. Moultos, C. Vega, Computation of electrical conductivities of aqueous electrolyte solutions: Two surfaces, one property, Journal of chemical theory and computation 19 (16) (2023) 5380–5393.
- [17] E. J. Maginn, R. A. Messerly, D. J. Carlson, D. R. Roe, J. R. Elliot, Best practices for computing transport properties 1. self-diffusivity and viscosity from equilibrium molecular dynamics [article v1. 0], Living Journal of Computational Molecular Science 1 (1) (2019) 6324–6324.
- [18] M. T. Humbert, Y. Zhang, E. J. Maginn, Pylat: Python lammps analysis tools, Journal of chemical information and modeling 59 (4) (2019) 1301–1305.
- [19] S. Chowdhuri, A. Chandra, Molecular dynamics simulations of aqueous nacl and kcl solutions: Effects of ion concentration on the single-particle, pair, and collective dynamical properties of ions and water molecules, The Journal of Chemical Physics 115 (8) (2001) 3732–3741.
- [20] L. Patro, O. Burghaus, B. Roling, Anomalous wien effects in supercooled ionic liquids, Physical review letters 116 (18) (2016) 185901.
- [21] L. Carbone, R. Verrelli, M. Gobet, J. Peng, M. Devany, B. Scrosati, S. Greenbaum, J. Hassoun, Insight on the li₂s electrochemical process in a composite configuration electrode, New Journal of Chemistry 40 (3) (2016) 2935–2943.

- [22] R. Kubo, Statistical-mechanical theory of irreversible processes. i. general theory and simple applications to magnetic and conduction problems, Journal of the physical society of Japan 12 (6) (1957) 570–586.
- [23] M. French, S. Hamel, R. Redmer, Dynamical screening and ionic conductivity in water from ab initio simulations, Physical review letters 107 (18) (2011) 185901.
- [24] R. Hafner, G. Guevara-Carrion, J. Vrabec, P. Klein, Sampling the bulk viscosity of water with molecular dynamics simulation in the canonical ensemble, The Journal of Physical Chemistry B 126 (48) (2022) 10172–10184.
- [25] R. Zwanzig, Time-correlation functions and transport coefficients in statistical mechanics, Annual Review of Physical Chemistry 16 (1) (1965) 67–102.
- [26] B. Doherty, X. Zhong, O. Acevedo, Virtual site opls force field for imidazolium-based ionic liquids, The Journal of Physical Chemistry B 122 (11) (2018) 2962–2974.
- [27] T. Darden, D. York, L. Pedersen, Particle mesh ewald: An n·log(n) method for ewald sums in large systems, The Journal of chemical physics 98 (12) (1993) 10089−10092.
- [28] B. Hess, H. Bekker, H. J. Berendsen, J. G. Fraaije, Lincs: A linear constraint solver for molecular simulations, Journal of computational chemistry 18 (12) (1997) 1463–1472.
- [29] M. J. Abraham, T. Murtola, R. Schulz, S. Páll, J. C. Smith, B. Hess, E. Lindahl, Gromacs: High performance molecular simulations through multi-level parallelism from laptops to supercomputers, SoftwareX 1 (2015) 19–25.
- [30] L. Martinez, R. Andrade, E. Birgin, J. Martinez, A package for building initial configurations for molecular dynamics simulations, J. Phys. Chem. Lett 30 (13) (2009) 92157–2164.
- [31] H. J. Berendsen, J. v. Postma, W. F. Van Gunsteren, A. DiNola, J. R. Haak, Molecular dynamics with coupling to an external bath, The Journal of chemical physics 81 (8) (1984) 3684–3690.

- [32] G. Bussi, D. Donadio, M. Parrinello, Canonical sampling through velocity rescaling, The Journal of chemical physics 126 (1) (2007).
- [33] D. J. Evans, B. L. Holian, The nose–hoover thermostat, The Journal of chemical physics 83 (8) (1985) 4069–4074.
- [34] M. Parrinello, A. Rahman, Polymorphic transitions in single crystals: A new molecular dynamics method, Journal of Applied physics 52 (12) (1981) 7182–7190.
- [35] C. Schreiner, S. Zugmann, R. Hartl, H. J. Gores, Fractional walden rule for ionic liquids: examples from recent measurements and a critique of the so-called ideal kcl line for the walden plot, Journal of Chemical & Engineering Data 55 (5) (2010) 1784–1788.
- [36] A. Noda, K. Hayamizu, M. Watanabe, Pulsed-gradient spin- echo 1h and 19f nmr ionic diffusion coefficient, viscosity, and ionic conductivity of non-chloroaluminate room-temperature ionic liquids, The Journal of Physical Chemistry B 105 (20) (2001) 4603–4610.
- [37] Q. Huang, T. C. Lourenço, L. T. Costa, Y. Zhang, E. J. Maginn, B. Gurkan, Solvation structure and dynamics of li⁺ in ternary ionic liquid–lithium salt electrolytes, The Journal of Physical Chemistry B 123 (2) (2018) 516–527.
- [38] Y.-H. Yu, A. N. Soriano, M.-H. Li, Heat capacities and electrical conductivities of 1-ethyl-3-methylimidazolium-based ionic liquids, The Journal of Chemical Thermodynamics 41 (1) (2009) 103–108.
- [39] T. Makino, M. Kanakubo, Y. Masuda, T. Umecky, A. Suzuki, Co₂ absorption properties, densities, viscosities, and electrical conductivities of ethylimidazolium and 1-ethyl-3-methylimidazolium ionic liquids, Fluid Phase Equilibria 362 (2014) 300–306.
- [40] K. R. Harris, M. Kanakubo, Self-diffusion coefficients and related transport properties for a number of fragile ionic liquids, Journal of Chemical & Engineering Data 61 (7) (2016) 2399–2411.